Solubility Isotherms of Systems Containing Optically Active Tris(ethylenediamine)cobalt(III) Ion. I. Reciprocal Salt-pairs, (Λ-$[Co(en)_3]^{3+}$, Δ-$[Co(en)_3]^{3+}$)-(Br^-, (*R*,*R*)-$C_4H_4O_6^{2-}$), at 25 °C

Akira Fuyuhiro,* Kazuaki Yamanari, and Yoichi Shimura
Department of Chemistry, Faculty of Science, Osaka University, Toyonaka, Osaka 560
(Received May 17, 1980)

A four-component solubility isotherm consisting of (Λ-$[Co(en)_3]^{3+}$, Δ-$[Co(en)_3]^{3+}$)-(Br^-, (*R*,*R*)-$C_4H_4O_6^{2-}$)-H_2O was determined at 25 °C. It was found that three double salts, *rac*-$[Co(en)_3]Br_3\cdot 3H_2O$, Λ-$[Co(en)_3]Br(d\text{-}C_4H_4O_6)\cdot 5H_2O$, and Λ-$[Co(en)_3]_{0.48}\cdot\Delta$-$[Co(en)_3]_{0.52}(d\text{-}C_4H_4O_6)_{1.5}\cdot 5H_2O$ and a gelatinous precipitate exist, six invariant points appearing. Application of this phase diagram to practical optical resolutions is discussed. The solubility of each salt in the system was measured in the range 5—65 °C in water, that of Λ- and Δ-$[Co(en)_3](d\text{-}C_4H_4O_6)_{1.5}\cdot nH_2O$ being found to be reversed at 42 °C.

A multi-component solubility isotherm containing chiral compounds is important for optical resolution, and those for some systems of metal complexes have been determined.[1,2] In the four-component systems of (Λ-$[Co(ox)(en)_2]^+$, Δ-$[Co(ox)(en)_2]^+$)-(Cl^-, R^-)-H_2O, where R^- denotes *d*-H_3tart^-, Δ-$[Co(edta)]^-$, or *d*-bcs$^-$(=(*R*,*R*)-$C_4H_6O_6$≡*d*-H_4tart and (1*R*,3*S*,4*S*,7*R*)-$C_{10}H_{14}OBrSO_3^-$≡*d*-bcs$^-$), optically inactive chloride ion does not participate in the formation of diastereomers or pseudoracemates, its introduction thus not playing any part in making optical resolution possible. On the other hand, in the system of $[Co(en)_3]^{3+}$ ion, optical resolution becomes possible by precipitating the diastereomer of double salt, Λ-$[Co(en)_3]Br(d\text{-}H_2tart)\cdot 5H_2O$.[3] It would be of interest to find the particular role of the fourth component, Br^-, in this optical resolution.

This paper deals with the determination of the solubility isotherm of reciprocal salt-pairs, (Λ-$[Co(en)_3]^{3+}$, Δ-$[Co(en)_3]^{3+}$)-(Br^-, *d*-H_2tart^{2-})-H_2O, at 25 °C, and of the solubility of *rac*-$[Co(en)_3]Br_3$, Λ-$[Co(en)_3]Br_3$, Λ- and Δ-$[Co(en)_3](d\text{-}H_2tart)_{1.5}$, and Λ-$[Co(en)_3]Br(d\text{-}H_2tart)$ at 5—65 °C.

Experimental

Materials. Λ-$[Co(en)_3]X$, $X=Br_3\cdot H_2O$, $Br(d\text{-}H_2tart)\cdot nH_2O$, *and* $(d\text{-}H_2tart)_{1.5}\cdot nH_2O$: The Λ-$[Co(en)_3]Br(d\text{-}H_2tart)\cdot 5H_2O$ diasteromer was prepared by the method of Werner,[3] partial asymmetric synthesis,[4] HCl being replaced by HBr, and by addition of equimolar amounts of HBr and *d*-H_4tart to a *rac*-$[Co(en)_3](OH)_3$ solution obtained by treating *rac*-$[Co(en)_3]Br_3$ with an anion exchange resin of OH^- form. Found: C, 21.44; H, 6.85; N, 15.08%. Calcd for Λ-$[Co(en)_3]Br(d\text{-}H_2tart)\cdot 5H_2O$: C, 21.55; H, 6.87; N, 15.08%. When a solution of the diastereomer was concentrated at *ca.* 60 °C, a monohydrated sample was obtained. Found: C, 24.67; H, 6.24; N, 17.32%. Calcd for Λ-$[Co(en)_3]Br(d\text{-}H_2tart)\cdot H_2O$: C, 24.75; H, 6.23; N, 17.32%. The Λ-$[Co(en)_3]Br_3\cdot H_2O$ complex was obtained by the method of Werner.[3] Found: C, 14.47; H, 5.30; N, 17.01%. Calcd for Λ-$[Co(en)_3]Br_3\cdot H_2O$: C, 14.50; H, 5.27; N, 16.91%. The diastereomer Λ-$[Co(en)_3](d\text{-}H_2tart)_{1.5}\cdot nH_2O$ was prepared from Λ-$[Co(en)_3]Br(d\text{-}H_2tart)\cdot 5H_2O$ and $Ag_2(d\text{-}H_2tart)$.[5] At first a paste-like solid precipitated from the solution, gradually turning into needles at room temperature. With a dilute solution the needles deposited directly. The needles are highly efflorescent. Crystallization from a solution at *ca.* 60 °C gave a hygroscopic 1.5-hydrated diastereomer. Found: C, 29.63; H, 6.83; N, 17.30%. Calcd for Λ-$[Co(en)_3](d\text{-}H_2tart)_{1.5}\cdot 1.5H_2O$: C. 29.51; H, 6.81; N, 17.21%.

Δ-$[Co(en)_3]X$, $X=Br_3\cdot H_2O$ *and* $(d\text{-}H_2tart)_{1.5}\cdot nH_2O$: The Δ-bromide monohydrate was prepared by adding 8 mol dm^{-3} HBr to the filtrate of the less soluble diastereomer Λ-$[Co(en)_3]Br(d\text{-}H_2tart)\cdot 5H_2O$. The bromide was optically purified by extraction into water at *ca.* 5 °C and repeated crystallization. Found: C, 14.51; H, 5.33; N, 16.96%. Calcd for Δ-$[Co(en)_3]Br_3\cdot H_2O$: C, 14.50; H, 5.27; N, 16.91%. The diastereomer Δ-$[Co(en)_3](d\text{-}H_2tart)_{1.5}\cdot nH_2O$ was prepared from Δ-$[Co(en)_3]Br_3\cdot H_2O$ and $Ag_2(d\text{-}H_2tart)$.[5] The prismatic crystals, highly efflorescent, have *ca.* 1.5—8 crystal waters. Found: C, 26.84; H, 7.11; N, 15.68%. Calcd for Δ-$[Co(en)_3](d\text{-}H_2tart)_{1.5}\cdot 4H_2O$: C, 27.02; H, 7.18; N, 15.76%.

rac-$[Co(en)_3]Br_3\cdot nH_2O$: Racemic bromide trihydrate was prepared by the method of Werner.[3] Found: C, 13.43; H, 5.69; N, 15.66%. Calcd for *rac*-$[Co(en)_3]Br_3\cdot 3H_2O$: C, 13.52; H, 5.67; N, 15.77%. Crystallization of the complex at *ca.* 60 °C gave a very hygroscopic monohydrate. Found: C, 14.40; H, 5.38; N, 16.97%. Calcd for *rac*-$[Co(en)_3]Br_3\cdot H_2O$: C, 14.50; H, 5.27; N, 16.91%.

Λ-$[Co(en)_3]_{0.48}\cdot\Delta$-$[Co(en)_3]_{0.52}(d\text{-}H_2tart)_{1.5}\cdot 5H_2O$: An apparent nonstoichiometric compound (not a mixture, see Results and Discussion) was prepared from *rac*-$[Co(en)_3]Br_3\cdot 3H_2O$ and $Ag_2(d\text{-}H_2tart)$ in a 2 : 3 mole ratio. Found: C, 26.16; H, 7.25; N, 15.26%. Calcd for $[Co(en)_3](d\text{-}H_2tart)_{1.5}\cdot 5H_2O$: C, 26.14; H, 7.31; N, 15.24%. The exact composition of the cations was determined by circular dichroism(CD)

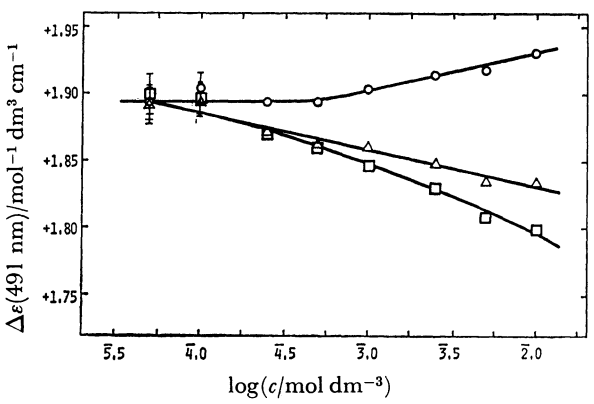

Fig. 1. Concentration dependence of $\Delta\varepsilon$(491 nm) in water.
○: Λ-$[Co(en)_3]Br_3$, △: Λ-$[Co(en)_3]Br(d\text{-}H_2tart)$, □: Λ-$[Co(en)_3](d\text{-}H_2tart)_{1.5}$.

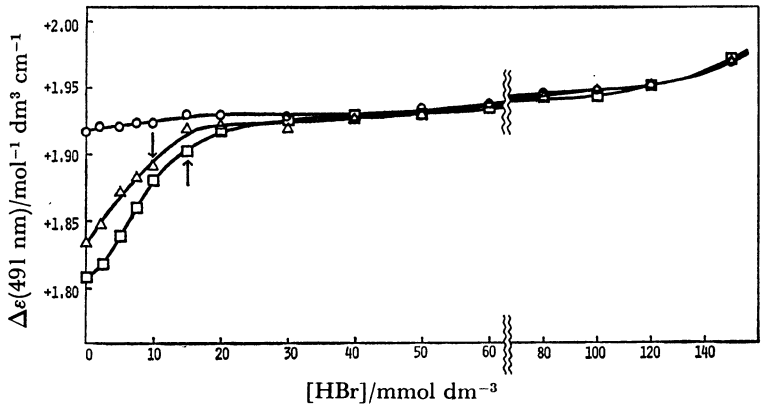

Fig. 2. CD in HBr aqueous solution. The concentration of Λ-$[Co(en)_3]^{3+}$ is 5 mmol dm^{-3}.
○: Λ-$[Co(en)_3]Br_3$, △: Λ-$[Co(en)_3]Br(d\text{-}H_2tart)$, □: Λ-$[Co(en)_3](d\text{-}H_2tart)_{1.5}$.

measurement in solution. The composition ($\Lambda : \Delta = 48\pm1 : 52\mp1$) was reproducible even by repeated recrystallization. Rapid cooling of the solution of $[Co(en)_3](d\text{-}H_2tart)_{1.5}$ sometimes provided a Λ-rich precipitate.

Measurements. *Calibrations of CD*: The molar absorption coefficient of $[Co(en)_3]^{3+}$ at the first d-d band(466 nm) was almost constant in spite of the presence of H^+, Br^-, and/or $d\text{-}H_2tart^{2-}$ in the concentration range 5×10^{-5}—10^{-2} mol dm^{-3} of the complex ion. Since the CD spectrum is considerably affected by the presence of $d\text{-}H_2tart^{2-}$ ion,[6] the influence of this ion on CD intensity was examined in water and in HBr solutions. The Λ-diastereomers, Λ-$[Co(en)_3]Br(d\text{-}H_2tart)$ and Λ-$[Co(en)_3](d\text{-}H_2tart)_{1.5}$, showed a gradual decrease in CD intensity with increase of complex concentration, and the $\Delta\varepsilon$ values at 10^{-2} mol dm^{-3} became 3 and 5% lower than the authentic value ($|\Delta\varepsilon(491\text{ nm})|=1.89$), respectively, the Λ-$[Co(en)_3]Br_3$ complex showing the reversed change (Fig. 1). The corresponding Δ-diastereomers, Δ-$[Co(en)_3]Br(d\text{-}H_2tart)$ and Δ-$[Co(en)_3](d\text{-}H_2tart)_{1.5}$, showed about half decreases in absolute values of $\Delta\varepsilon$ as compared with Λ-diastereomers in the concentration range 5×10^{-5}—10^{-2} mol dm^{-3}. The CD intensities depend a great deal upon the complex concentration in water. Figure 2 shows the variations of CD intensity at 491 nm in HBr solutions. In both systems of Λ-$[Co(en)_3]Br(d\text{-}H_2tart)$ and Λ-$[Co(en)_3](d\text{-}H_2tart)_{1.5}$, the CD intensities were almost constant in HBr solutions (2×10^{-2}—10^{-1} mol dm^{-3}) in Fig. 2, where the arrows indicate the points at which $d\text{-}H_2tart^{2-}$ should exist in acid form $d\text{-}H_4tart$ if we neglect the acid dissociations. The corresponding Δ-diastereomers showed about 2/3 increase in absolute values of $\Delta\varepsilon$ between [HBr]=0 and the plateau as compared with the Λ-diastereomers. Figures 3 and 4 show the concentration dependence of induced CD of *rac*-$[Co(en)_3](d\text{-}H_2tart)_{1.5}$ in water and in HBr solutions, respectively. Since the complex could not be obtained as a solid, the reaction mixture was used in solution, its concentration being determined by optical density. The induced CD peak appears at 461 nm,[6] but the measurements were carried out at 491 nm. Measurements in HBr solutions were found to be more favorable than in water because the CD intensities are almost zero in an appropriate HBr solution irrespective of the complex concentration. Beer's law holds in the concentration range 0—10^{-2} mol dm^{-3} in a 5×10^{-2} mol dm^{-3} HBr aqueous solution.

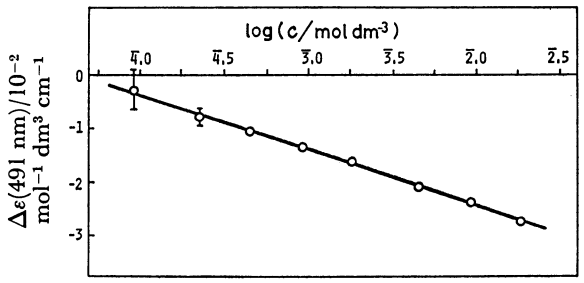

Fig. 3. Concentration dependence of induced CD of *rac*-$[Co(en)_3](d\text{-}H_2tart)_{1.5}$ in water at 491 nm.

Analyses of Saturated Solutions: Solubility in water was determined in molality.[1] Saturated solution weighed was diluted with a 5×10^{-2} mol dm^{-3} HBr aqueous solution to a certain volume. Optical densities and CD were measured under the conditions described above. The concentrations of $\{\Lambda\text{-}[Co(en)_3]^{3+}+\Delta\text{-}[Co(en)_3]^{3+}\}$ were determined from the

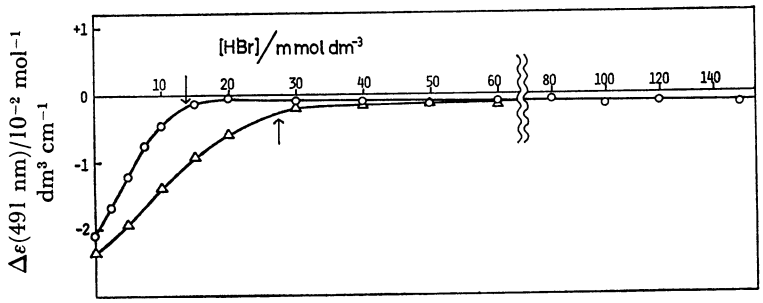

Fig. 4. Induced CD of *rac*-$[Co(en)_3](d\text{-}H_2tart)_{1.5}$ (○; 4.62 mmol dm^{-3} and △; 9.17 mmol dm^{-3}) in HBr aqueous solution.

observed optical densities, referring to the calibrated molar absorption coefficient of $[Co(en)_3]^{2+}$, $\varepsilon(466\,nm)=91.0$, the concentrations of $\{\Lambda\text{-}[Co(en)_3]^{3+}-\Delta\text{-}[Co(en)_3]^{3+}\}$ being obtained from CD intensities calibrated above; $\Delta\varepsilon(491\,nm)=+1.93$ and -1.93 for Λ- and Δ-$[Co(en)_3]^{3+}$, respectively. The concentrations of Λ- and Δ-$[Co(en)_3]^{3+}$ were separately calculated from the concentrations of $\{\Lambda\text{-}[Co(en)_3]^{3+}+\Delta\text{-}[Co(en)_3]^{3+}\}$ and $\{\Lambda\text{-}[Co(en)_3]^{3+}-\Delta\text{-}[Co(en)_3]^{3+}\}$. In the presence of both Br^- and d-H_2tart^{2-} ions, a titration method was combined with the spectral one in order to determine the amount of Br^-. A saturated solution was taken, weighed and diluted with an appropriate amount of water. The solution was titrated with a 0.03 mol dm^{-3} $AgNO_3$ solution till the end point of precipitation of AgBr, which was followed by the electromotive force(e.m.f.) of the following chemical cell: Ag|sample||KNO_3 soln.||3.33 mol dm^{-3} KCl soln.|AgCl(s)|Ag. The e.m.f. jumped distinctly between the precipitation of AgBr and $Ag_2(d\text{-}H_2tart)$, and the end point was calibrated by the known amounts of NaBr, Λ- and *rac*-$[Co(en)_3]Br_3\cdot nH_2O$, Λ-$[Co(en)_3]Br(d\text{-}H_2tart)\cdot 5H_2O$, and Λ- and Δ-$[Co(en)_3](d\text{-}H_2tart)_{1.5}\cdot nH_2O$. In the binary systems the concentration could be derived from only the optical densities. In this way, the amounts of all cations and anions and then the amount of water in the saturated solution were obtained and given in molality.

Analyses of Solid Phases: The solid phases were identified from elemental analyses, absorption and CD spectra, gravimetric analyses, and differential thermal analyses(DTA). The DTA were performed under dry or suspended (in water) conditions at atmospheric pressure. Optical densities were measured with a JASCO UVIDEC-1 spectrophotometer and CD with a JASCO MOE-1 spectropolarimeter.

Results and Discussion

The solubility data are given in Tables 1 and 2, and Figs. 5—11. A saturated solution is expressed as a point defined by summing up the position vectors of the solubilities of the component salt(s) contained.[1)]

Binary Systems between 5 and 65 °C. Figure 5 shows the binary solubility curves of the complexes, a few points of solubility of which have been reported.[5,7)] The more the tartrate ion share in the counter ions, the steeper the slopes of solubility curves. The solubility of Λ-$[Co(en)_3](d\text{-}H_2tart)_{1.5}$ at 60 °C in particular is about 90 times greater than that at 5 °C. The solubility of a pair of diastereomers, Λ- and Δ-$[Co(en)_3](d\text{-}H_2tart)_{1.5}$ is reversed at 42 °C; the Λ-diastereomer is less soluble at temperatures below 42 °C and the Δ above 42 °C. Inflection points were observed in *rac*-[Co-

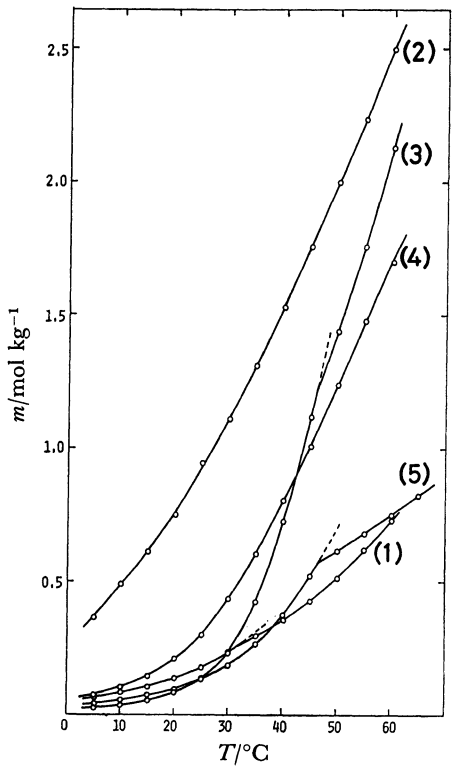

Fig 5. Solubility curves, where solubility is presented in molality m of anhydrous salt. (1): *rac*-$[Co(en)_3]Br_3\cdot nH_2O$, $n=3(\lesssim 32\,°C)$ and $n\simeq 1(\gtrsim 32\,°C)$, (2): Λ-$[Co(en)_3]Br_3\cdot H_2O$, (3): Λ-$[Co(en)_3](d\text{-}H_2tart)_{1.5}\cdot nH_2O$, $n\gtrsim 7(\lesssim 47\,°C)$ and $n\simeq 1.5(\gtrsim 47\,°C)$, (4): Δ-$[Co(en)_3](d\text{-}H_2tart)_{1.5}\cdot nH_2O$, $n\simeq 8$, (5): Λ-$[Co(en)_3]Br(d\text{-}H_2tart)\cdot nH_2O$, $n=5(\lesssim 47\,°C)$ and $n=1(\gtrsim 47\,°C)$.

Table 1. Solubility of the $[Co(en)_3]^{3+}$ salts in water (molality m/mol kg^{-1} of anhydrous salt)

T/°C	No. of salt[a)]							
	(1)-α	(1)-β	(2)	(3)-α	(3)-β	(4)	(5)-α	(5)-β
5	0.0629		0.363	0.0236		0.0729	0.0402	
10	0.0820		0.491	0.0351		0.103	0.0540	
15	0.107		0.613	0.0538		0.145	0.0736	
20	0.138		0.751	0.0847		0.210	0.0981	
25	0.178		0.947	0.138		0.299	0.135	
30	0.231		1.11	0.237		0.436	0.187	
35		0.295	1.31	0.422		0.604	0.263	
40		0.356	1.53	0.727		0.807	0.374	
45		0.428	1.76	1.12		1.01	0.522	
50		0.514	2.00		1.44	1.24		0.619
55		0.622	2.24		1.76	1.49		0.681
60		0.734	2.50		2.13	1.70		0.750
65		—	—		—	—		0.825

a) (1) *rac*-$[Co(en)_3]Br_3\cdot nH_2O$, $n=3(\alpha)$ and $n\simeq 1(\beta)$; (2) Λ-$[Co(en)_3]Br_3\cdot H_2O$; (3) Λ-$[Co(en)_3](d\text{-}H_2tart)_{1.5}\cdot nH_2O$, $n\gtrsim 7(\alpha)$ and $n\simeq 1.5(\beta)$; (4) Δ-$[Co(en)_3](d\text{-}H_2tart)_{1.5}\cdot nH_2O$, $n\simeq 8$; (5) Λ-$[Co(en)_3]Br(d\text{-}H_2tart)\cdot nH_2O$, $n=5(\alpha)$ and $n=1(\beta)$.

TABLE 2. EQUILIBRIUM OF (Λ-$[Co(en)_3]^{3+}$, Δ-$[Co(en)_3]^{3+}$)-(Br^-, d-H_2tart^{2-})-H_2O SYSTEM AT 25 °C

In liquid phases, solubility is presented in molality m of the component ions. Abbreviations are as follows: Λ-$[Co(en)_3]^{3+}=\Lambda^{3+}$, Δ-$[Co(en)_3]^{3+}=\Delta^{3+}$, Λ-$[Co(en)_3]Br_3\cdot H_2O=\Lambda Br_3$, Δ-$[Co(en)_3]Br_3\cdot H_2O=\Delta Br_3$, *rac*-$[Co(en)_3]Br_3\cdot 3H_2O=\Lambda\Delta Br_6$, Λ-$[Co(en)_3]Br(d\text{-}H_2tart)\cdot 5H_2O=\Lambda Br(tart)$, Λ-$[Co(en)_3](d\text{-}H_2tart)_{1.5}\cdot nH_2O$ ($n\gtrsim 7$)$=\Lambda(tart)_{1.5}$, Δ-$[Co(en)_3]$ (d-$H_2tart)_{1.5}\cdot nH_2O$ ($n\simeq 8$)$=\Delta(tart)_{1.5}$, and Λ-$[Co(en)_3]_{0.48}\cdot\Delta$-$[Co(en)_3]_{0.52}$-($d$-$H_2tart)_{1.5}\cdot 5H_2O=(\Lambda,\Delta)(tart)_{1.5}$. The gelatinous precipitate(Gela) is treated as solid.

Position of points (Figs. 6—11)	No. of components	Liquid phase[a] $m/10^{-1}$ mol kg^{-1} Λ^{3+}	Δ^{3+}	Br^-	Solid phase
A	2	9.47 (±0.08)		28.4 (±0.2)	ΛBr_3
E_3	2	0.892 (±0.010)	0.892 (±0.010)	5.35 (±0.06)	$\Lambda\Delta Br_6$
E_3 ↕ E_1	3	1.01 1.15 1.38 2.20 3.59 5.29 6.06 7.52	0.77 0.70 0.52 0.22 0.08 0.08 0.00 0.00	5.36 5.53 5.69 7.25 11.0 15.9 18.2 22.6	$\Lambda\Delta Br_6$
E_1	3	9.63 (±0.16)	0.00	28.9 (±0.5)	ΛBr_3 +$\Lambda\Delta Br_6$
E_3 ↕ E_2	3	0.808 0.70 0.48 0.14 0.03 0.01 0.00 0.00	0.990 1.14 1.47 2.56 4.26 6.11 7.00 8.75	5.39 5.52 5.86 8.10 12.9 18.4 21.0 26.3	$\Lambda\Delta Br_6$
E_2	3	0.00	9.63 (±0.16)	28.9 (±0.5)	ΔBr_3 +$\Lambda\Delta Br_6$
B	2		9.47 (±0.08)	28.4 (±0.2)	ΔBr_3
C	2		2.99 (±0.04)		$\Delta(tart)_{1.5}$
D	2	1.38 (±0.02)			$\Lambda(tart)_{1.5}$
D ↕ G_1	3	1.39 1.42 1.45	0.07 0.12 0.16		$\Lambda(tart)_{1.5}$
G_1	3	1.47 (±0.02)	0.20 (±0.02)		$(\Lambda,\Delta)(tart)_{1.5}$ +$\Lambda(tart)_{1.5}$
G_1 ↕ G_2	3	1.36 1.28 1.12 1.00 0.967 0.964 0.956 0.916 0.832 0.810 0.774 0.731 0.626 0.500 0.468	0.20 0.20 0.21 0.23 0.252 0.250 0.246 0.248 0.268 0.277 0.280 0.295 0.340 0.414 0.450		$(\Lambda,\Delta)(tart)_{1.5}$
G_1 ↕ G_2	3	0.430 0.368 0.369 0.305 0.252 0.21 0.20 0.18 0.17 0.16 0.14 0.14 0.13 0.12 0.11 0.11 0.10 0.11	0.479 0.550 0.568 0.689 0.856 1.05 1.20 1.37 1.47 1.66 1.81 2.03 2.26 2.45 2.59 2.71 2.74 2.83		$(\Lambda,\Delta)(tart)_{1.5}$
G_2	3	0.10 (±0.01)	3.09 (±0.07)		$(\Lambda,\Delta)(tart)_{1.5}$ +$\Delta(tart)_{1.5}$
D ↕ H_1	3	1.45 1.57 1.71 1.84 2.00		0.09 0.25 0.44 0.62 0.81	$\Lambda(tart)_{1.5}$
H_1	3	2.15 (±0.02)		1.02 (±0.04)	$\Lambda(tart)_{1.5}$ +$\Lambda Br(tart)$
H_1 ↕ H_3	3	2.07 2.00 1.99 1.80 1.72 1.65 1.64 1.52 1.43 1.39 1.37		1.02 1.05 1.03 1.08 1.16 1.12 1.14 1.19 1.24 1.29 1.32	$\Lambda Br(tart)$
H_3	2	1.35 (±0.01)		1.35 (±0.01)	$\Lambda Br(tart)$
H_3 ↕ H_2	3	1.30 1.28 1.28 1.26 1.24 1.23 1.21 1.24 1.27 1.24 1.38 1.50		1.42 1.46 1.49 1.54 1.57 1.68 1.79 1.91 2.24 2.23 2.72 3.19	$\Lambda Br(tart)$

TABLE 2. (Continued)

Position of points (Figs. 6—11)	No. of components	Liquid phase[a] $m/10^{-1}$ mol kg^{-1} A^{3+}	Δ^{3+}	Br^-	Solid phase
		1.66		3.78	
		1.98		4.79	
		2.31		5.78	
		2.39		5.95	
		2.47		6.21	
H_3		2.72		6.96	
↑		3.37		8.85	
	3	4.03		10.8	ABr(tart)
↓		5.09		13.8	
		5.66		15.6	
H_2		6.09		16.5	
		6.40		17.5	
		7.40		20.1	
		7.42		20.4	
		8.30		22.9	
		8.89		24.7	
H_2	3	10.9 (±0.2)		30.3 (±0.7)	ABr(tart) + ABr$_3$
A		9.67		28.4	
↑		9.91		28.7	
	3	9.99		28.8	ABr$_3$
↓		10.3		29.5	
H_2					
E_1		10.5	0.0	29.9	ABr$_3$
↕	4				
P_1		11.2	0.0	31.0	+ $A\Delta$Br$_6$
P_1	4	10.9 (±0.2)	0.0	30.6 (±0.9)	ABr(tart) + ABr$_3$ + $A\Delta$Br$_6$
		8.11	0.02	22.3	
		7.32	0.01	20.1	
		6.92	0.03	19.0	
		4.91	0.05	13.4	
		4.24	0.11	11.7	
		3.80	0.13	10.3	
		3.00	0.24	8.32	
		2.64	0.33	7.48	
		2.27	0.50	6.78	
		2.19	0.54	6.70	
		2.16	0.64	6.81	
P_1		2.06	0.65	6.51	
↑		2.02	0.76	6.62	ABr(tart)
	4	1.84	0.98	6.53	
↓		1.69	1.18	6.53	+ $A\Delta$Br$_6$
		1.61	1.39	6.53	
P_4		1.54	1.58	6.65	
		1.50	1.73	6.68	
		1.48	1.85	6.85	
		1.44	2.18	7.08	
		1.41	2.44	7.36	
		1.43	2.35	7.24	
		1.42	2.39	7.20	
		1.40	2.73	7.56	
		1.37	3.46	8.37	
		1.38	3.87	8.73	
		1.40	3.97	8.87	
P_1		1.41	4.38	9.19	
↕	4	1.43	4.82	9.64	ABr(tart) + $A\Delta$Br$_6$
P_4		1.45	5.83	10.7	
P_4	4	1.51 (±0.01)	6.89 (±0.08)	11.8 (±0.3)	ABr(tart) + $A\Delta$Br$_6$ + Gela
G_1		1.61	0.21	0.20	(A,Δ)(tart)$_{1.5}$
↕	4				
P_2		2.07	0.27	0.87	+ A(tart)$_{1.5}$
H_1		2.23	0.18	1.06	A(tart)$_{1.5}$
↕	4				
P_2		2.23	0.19	1.07	+ ABr(tart)
P_2	4	2.28 (±0.03)	0.29 (±0.01)	1.12 (±0.03)	(A,Δ)(tart)$_{1.5}$ + A(tart)$_{1.5}$ + ABr(tart)
		2.06	0.33	1.20	
		2.02	0.33	1.20	
		1.91	0.36	1.23	
		1.79	0.40	1.30	
		1.73	0.42	1.36	
		1.73	0.43	1.40	
		1.72	0.44	1.38	
		1.69	0.45	1.39	
		1.68	0.47	1.44	
		1.65	0.47	1.46	
		1.62	0.49	1.48	
		1.59	0.52	1.52	
P_2		1.55	0.55	1.61	
↑		1.52	0.57	1.62	(A,Δ)(tart)$_{1.5}$
	4	1.47	0.64	1.72	
		1.43	0.72	1.81	+ ABr(tart)
↓		1.41	0.75	1.87	
P_5		1.37	0.82	2.00	
		1.35	0.91	2.14	
		1.33	1.01	2.27	
		1.30	1.15	2.49	
		1.30	1.17	2.60	
		1.30	1.19	2.55	
		1.29	1.32	2.77	
		1.27	1.46	3.01	
		1.26	1.89	3.63	
		1.26	2.30	4.25	
		1.29	2.66	4.77	
		1.30	3.09	5.42	
P_5	4	1.36 (±0.02)	4.12 (±0.19)	6.99 (±0.27)	(A,Δ)(tart)$_{1.5}$ + ABr(tart) + Gela
				9.89	29.1	
				10.4	29.8	
B				11.4	31.3	
↑				12.5	33.0	
	3			13.4	34.0	ΔBr$_3$
↓				14.1	35.0	
				14.7	35.7	
F_2				14.5	35.0	
				14.4	35.2	

Table 2. (Continued)

Position of points (Figs. 6—11)	No. of components	Liquid phase[a] $m/10^{-1}$ mol kg^{-1} Λ^{3+}	Δ^{3+}	Br^-	Solid phase
F_2	3		15.4 (±0.4)	36.5 (±0.7)	ΔBr_3 +Gela
E_2 ↑ ↓ P_3	4	0.0	10.4	29.8	
		0.0	11.3	31.4	
		0.0	12.1	32.5	
		0.0	12.8	33.4	ΔBr_3
		0.0	13.5	34.1	$+\Lambda\Delta Br_6$
		0.0	14.0	34.6	
		0.0	14.8	36.2	
		0.0	15.5	36.5	
P_3	4	0.0	15.8 (±0.2)	36.0 (±0.2)	ΔBr_3 $+\Lambda\Delta Br_6$ +Gela
C ↑ ↓ F_1	3		3.39	0.41	
			3.82	0.90	
			4.59	1.65	$\Delta(tart)_{1.5}$
			5.66	2.88	
			6.62	4.02	
F_1	3		6.91 (±0.29)	4.40 (±0.35)	$\Delta(tart)_{1.5}$ +Gela
G_2 ↑ ↓ P_6	4	0.11	3.57	0.60	
		0.13	4.33	1.42	
		0.16	5.09	2.33	$(\Lambda,\Delta)(tart)_{1.5}$ $+\Delta(tart)_{1.5}$
		0.17	5.70	3.08	
		0.18	6.55	3.93	
P_6	4	0.21 (±0.03)	7.11 (±0.24)	4.66 (±0.31)	$(\Lambda,\Delta)(tart)_{1.5}$ $+\Delta(tart)_{1.5}$ +Gela

a) Values in parentheses are estimated errors and calculated from twice the standard deviations of measurements repeated 3—14 times.

$(en)_3]Br_3$, Λ-$[Co(en)_3]Br(d\text{-}H_2tart)$, and Λ-$[Co(en)_3]$-$(d\text{-}H_2tart)_{1.5}$ at about 32, 47, and 47 °C, respectively. The points were also clearly observed by DTA. Under dry conditions these three complexes provided no DTA peak at the inflection points, the peaks being observed under suspended conditions in water. The *rac*-$[Co(en)_3]Br_3\cdot nH_2O$ salt showed the peak in both heating and cooling processes, Λ-$[Co(en)_3]Br(d\text{-}H_2tart)\cdot nH_2O$ and Λ-$[Co(en)_3](d\text{-}H_2tart)_{1.5}\cdot nH_2O$ only in heating process. The Λ-$[Co(en)_3]Br(d\text{-}H_2tart)$ salt in high temperature form were gradually transformed into low temperature form in 1—3 h at room temperature, the latter giving the DTA peak again on heating. It took a few days for Λ-$[Co(en)_3](d\text{-}H_2tart)_{1.5}$ to be transformed into low temperature form, the change corresponding to the transfer of the paste-like precipitate to the needles (see Experimental).

The Ternary System, Λ-$[Co(en)_3]Br_3$–Δ-$[Co(en)_3]Br_3$–H_2O. The solubility isotherm of this type determines whether the racemate is spontaneously resolved or not.[8,9] Figure 6 shows the solubility isotherm of the ternary system, Λ-$[Co(en)_3]Br_3$–Δ-$[Co(en)_3]Br_3$–H_2O, at 25 °C. Points A, B, and E_3 indicate the binary solubility of Λ-, Δ-, and *rac*-$[Co(en)_3]Br_3\cdot nH_2O$, respectively, no spontaneous resolution taking place. In this system, two invariant points, E_1 and E_2, appear and the widely spread curve, $E_1E_3E_2$, represents the solubility isotherm of the racemic compound, *rac*-$[Co(en)_3]Br_3\cdot 3H_2O$. Point $E_1(E_2)$ lies extremely close to the left(right) axis, optical purity of the liquid phase at E_1 and E_2 being almost perfect. A similar ternary system, Λ-$[Co(ox)(en)_2]I$–Δ-$[Co(ox)(en)_2]I$–H_2O,[9] is not so extreme as the present system.

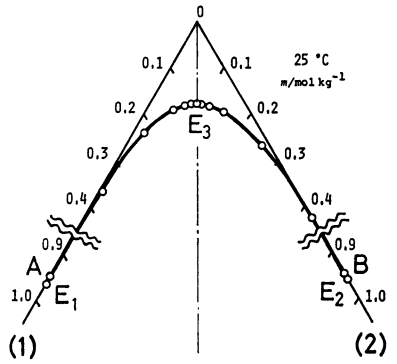

Fig. 6. Solubility isotherm of the ternary system, Λ-$[Co(en)_3]Br_3$–Δ-$[Co(en)_3]Br_3$–H_2O, at 25 °C.
Solubility is presented in molality m of anhydrous salt. (1): Λ-$[Co(en)_3]Br_3$, (2): Δ-$[Co(en)_3]Br_3$.

The Ternary System, Λ-$[Co(en)_3](d\text{-}H_2tart)_{1.5}$–$\Delta$-$[Co(en)_3](d\text{-}H_2tart)_{1.5}$–$H_2O$. The solubility isotherm of this type which consists of a pair of diastereomers and solvent is the simplest one for discussion of optical resolution. Figure 7 shows the system, Λ-$[Co(en)_3]$-$(d\text{-}H_2tart)_{1.5}$–Δ-$[Co(en)_3](d\text{-}H_2tart)_{1.5}$–$H_2O$, at 25 °C. This resembles those of the following systems, Λ-$[Co(ox)(en)_2]R$–Δ-$[Co(ox)(en)_2]R$–H_2O (25 °C); $R^- = 1/2\text{-}[Sb_2(d\text{-}tart)_2]^{2-}$ and *d*-bcs$^-$, in which the pseudoracemic compounds, Λ-$[Co(ox)(en)_2]\cdot\Delta$-$[Co(ox)(en)_2]\cdot[Sb_2(d\text{-}tart)_2]\cdot 5H_2O$ and Λ-$[Co(ox)(en)_2]\cdot\Delta$-$[Co(ox)(en)_2](d\text{-}bcs)_2\cdot 2H_2O$, respectively, are formed between

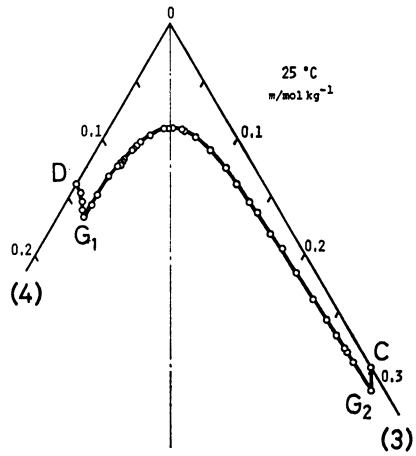

Fig. 7. Solubility isotherm of the ternary system, Λ-$[Co(en)_3](d\text{-}H_2tart)_{1.5}$–$\Delta$-$[Co(en)_3](d\text{-}H_2tart)_{1.5}$–$H_2O$, at 25 °C.
Solubility is presented in molality m of anhydrous salt. (4): Λ-$[Co(en)_3](d\text{-}H_2tart)_{1.5}$, (3): Δ-$[Co(en)_3]$-$(d\text{-}H_2tart)_{1.5}$.

the two diastereomers.[9,10] However, the ratio of *Λ*: *Δ* in the central solid phase of the present system is not 50 : 50% but (48±1) : (52∓1)% on the curve G_1G_2 (Fig. 7). Since the effect of induced CD exerts less than 0.1% for deviation of this ratio (see Experimental), it is reasonable to conclude that the compound is a nonstoichiometric substance with the composition *Λ*-$[Co(en)_3]_{0.48}$·*Δ*-$[Co(en)_3]_{0.52}$(*d*-H_2tart)$_{1.5}$·$5H_2O$. The compound (not mixture) might correspond to the precipitate prepared from a mixed solution of *rac*-$[Co(en)_3]X_3$ (X=Cl and Br) and KNa(*d*-H_2tart) by addition of ethanol.[11] If we attempt optical resolution with this ternary system, *viz.*, a solution of $[Co(en)_3]$-(*d*-H_2tart)$_{1.5}$ is concentrated at 25 °C, only a partially resolved *compound* will be obtained. Thus we must treat a four-component system to resolve the $[Co(en)_3]^{3+}$ complex perfectly.

The Ternary System, Λ-[Co(en)$_3$](d-H$_2$tart)$_{1.5}$–Λ-[Co(en)$_3$]Br$_3$–H$_2$O. Figure 8 shows the isotherm at

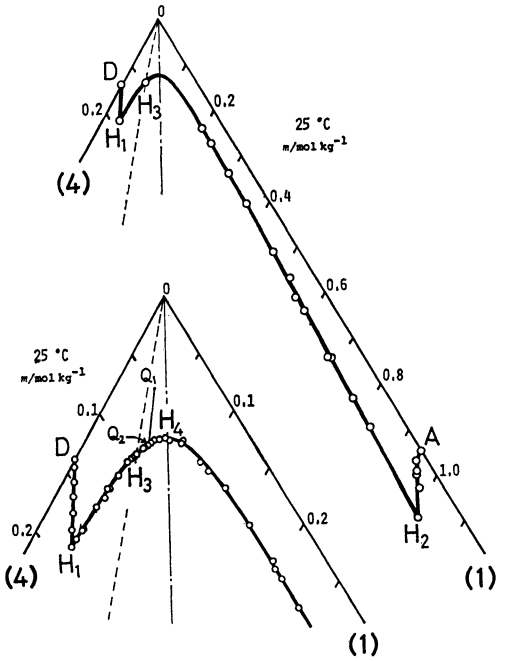

Fig. 8. Solubility isotherm (upper) and its magnification of the ternary system, *Λ*-$[Co(en)_3]$(*d*-H_2tart)$_{1.5}$–*Λ*-$[Co(en)_3]Br_3$–H_2O, at 25 °C.
Solubility is presented in molality *m* of anhydrous salt.
(4): *Λ*-$[Co(en)_3]$(*d*-H_2tart)$_{1.5}$, (1): *Λ*-$[Co(en)_3]Br_3$.

25 °C which is irrelevant to a successful optical resolution. Points D, H_3, and A denote the solubility of binary systems, *Λ*-$[Co(en)_3]$(*d*-H_2tart)$_{1.5}$, *Λ*-$[Co(en)_3]$Br-(*d*-H_2tart), and *Λ*-$[Co(en)_3]Br_3$, respectively. Since the central solid has the composition *Λ*-$[Co(en)_3]$Br(*d*-tart)·$5H_2O$, the point of this solid exists on the elongation of line OH_3. The liquid phase composition of minimum solubility of *Λ*-$[Co(en)_3]^{3+}$ corresponds to point H_4 where the ratio of *Λ*-$[Co(en)_3]$(*d*-H_2tart)$_{1.5}$: *Λ*-$[Co(en)_3]Br_3$ is equal to 1 : 1, or (*d*-H_2tart)$^{2-}$: Br^- to 1 : 2, but not to 1 : 1 which agrees with point H_3. When an unsaturated solution of Q_1 is concentrated at 25 °C, the salt *Λ*-$[Co(en)_3]$Br(*d*-H_2tart)·$5H_2O$ will deposit at Q_2 and the composition of the saturated solution will concomitantly move toward the minimum solubility of *Λ*-$[Co(en)_3]^{3+}$(H_4), and in turn, to the point H_2 where two solids, *Λ*-$[Co(en)_3]$Br(*d*-H_2tart)·$5H_2O$ and *Λ*-$[Co(en)_3]Br_3$·H_2O, coexist.

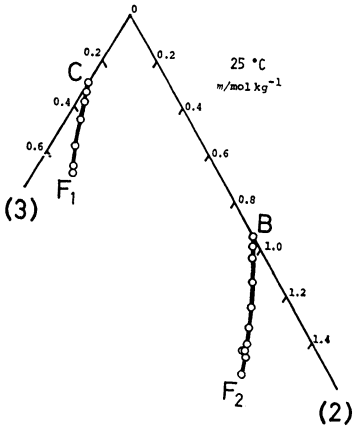

Fig. 9. Solubility isotherm of the ternary system, *Δ*-$[Co(en)_3]$(*d*-H_2tart)$_{1.5}$–*Δ*-$[Co(en)_3]Br_3$–H_2O, at 25 °C.
Solubility is presented in molality *m* of anhydrous salt.
(3): *Δ*-$[Co(en)_3]$(*d*-H_2tart)$_{1.5}$, (2): *Δ*-$[Co(en)_3]Br_3$.

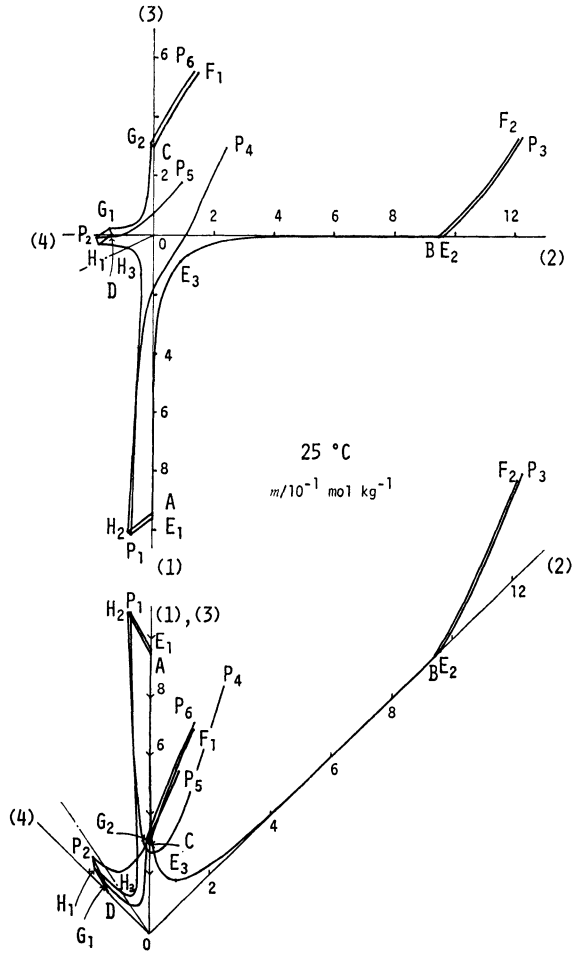

Fig. 10. The plane projection(upper) and the side elevation of solubility isotherm of the system, (*Λ*-$[Co(en)_3]^{3+}$, *Λ*-$[Co(en)_3]^{3+}$)-(Br^-, *d*-H_2tart^{2-})-H_2O, at 25 °C.
Solubility is presented in molality *m* of anhydrous salt.
(1): *Λ*-$[Co(en)_3]Br_3$, (2): *Δ*-$[Co(en)_3]Br_3$, (3): *Δ*-$[Co(en)_3]$(*d*-H_2tart)$_{1.5}$, (4): *Λ*-$[Co(en)_3]$(*d*-H_2tart)$_{1.5}$.

The Ternary System, Δ-[*Co(en)*$_3$](d-*H*$_2$*tart*)$_{1.5}$–Δ-[*Co(en)*$_3$]*Br*$_3$–*H*$_2$*O*. As shown in Fig. 9, the central part of the isotherm is blank owing to the appearance of gelatinous substances; when measurements of the saturated solutions from points C and B were carried out to points F_1 and F_2, respectively, the liquid phase turned into a gelatinous substance. This was obtained from the filtrate of the optical resolution and reported as *Δ*-[Co(en)$_3$]Br(*d*-H_2tart)·5H_2O,[3] but the composition and structure have not been determined clearly.

The lines DG_1, CG_2, DH_1, AH_2, CF_1, and BF_2 in Figs. 7—9 go down almost vertically. The situation differs significantly from the one expected from the common ion effect, suggesting that the activity coefficient of each salt becomes very small because of the association between $[Co(en)_3]^{3+}$ and *d*-H_2tart^{2-}.

*The Solubility Isotherm of Reciprocal Salt-pairs, (*Λ-[*Co(en)*$_3$]$^{3+}$, Δ-[*Co(en)*$_3$]$^{3+}$*)-(Br*$^-$, d-*H*$_2$*tart*$^{2-}$*)-H*$_2$*O*. The solubility isotherm of reciprocal salt-pairs consisting

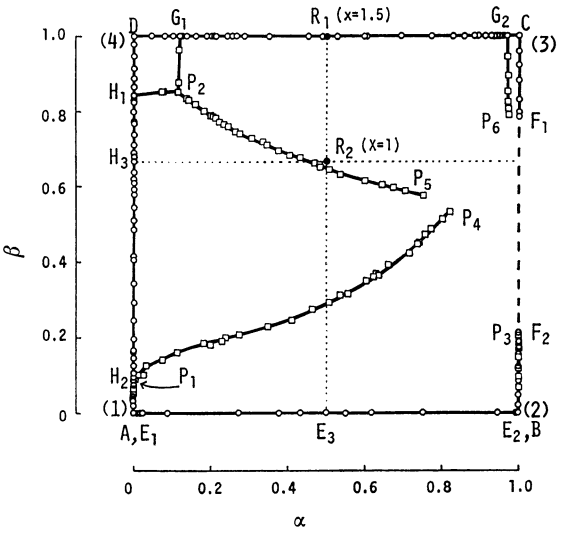

Fig. 11. The clinographic projection of solubility isotherm of the system, (*Λ*-[Co(en)$_3$]$^{3+}$, *Δ*-[Co(en)$_3$]$^{3+}$)-(Br$^-$, *d*-H_2tart^{2-})-H_2O, at 25 °C.
α: mole fraction of *Δ*-[Co(en)$_3$]$^{3+}$ to all the cations, β: mole fraction of (*d*-$H_2tart)_{1.5}^{3-}$ to {$(Br_3)^{3-}$+(*d*-H_2-tart)$_{1.5}^{3-}$}, (1): *Λ*-[Co(en)$_3$]Br_3, (2): *Δ*-[Co(en)$_3$]Br_3, (3): *Δ*-[Co(en)$_3$](*d*-$H_2tart)_{1.5}$, (4): *Λ*-[Co(en)$_3$](*d*-H_2-tart)$_{1.5}$, □: solubilities of four-components, ○: solubilities of two- or three-components.

of two cations, two anions, and solvent can be drawn in space and projected on three planes according to the definition[1] in which solubility is expressed in molality of component ions and then the molality of three salts. In the present system, the charges of the component anions differ, molalities of Br^- and *d*-H_2tart^{2-} being calculated as those of $(Br_3)^{3-}$ and (*d*-$H_2tart)_{1.5}^{3-}$, respectively. The four-component system includes the ternary systems in the above sections. The plane projection and side elevation are shown in Fig. 10 and the clinographic projection of the isotherm at 25 °C in Fig. 11. The left, right, lower, and upper sides in Fig. 11 correspond to Figs. 8, 9, 6, and 7, respectively. There are three double salts, *Λ*-[Co(en)$_3$]·*Δ*-[Co(en)$_3$]Br_6·6H_2O(=*rac*-[Co(en)$_3$]Br_3·3H_2O), *Λ*-[Co(en)$_3$]Br(*d*-H_2-tart)·5H_2O, and *Λ*-[Co(en)$_3$]$_{0.48}$·*Δ*-[Co(en)$_3$]$_{0.52}$(*d*-$H_2tart)_{1.5}$·5H_2O and one gelatinous precipitate in the areas $E_1E_3E_2P_3P_4P_1E_1$, $H_1H_3H_2P_1P_4P_5P_2H_1$, $G_1P_2P_5P_6$-G_2G_1, and $F_2F_1P_6P_5P_4P_3F_2$, respectively. In this system six invariant points, P_1—P_6, having four components exist at 25 °C. Since the *Λ*-[Co(en)$_3$]Br(*d*-H_2tart)·5H_2O diastereomer covers the area across the "racemic line" R_1E_3 (Fig. 11), the perfect optical resolution of $[Co(en)_3]^{3+}$ ion is possible by using Br^- and *d*-H_2tart^{2-} as resolving agents at 25 °C. However, it should be noted that the saturated solution of *rac*-[Co(en)$_3$]Br(*d*-H_2tart) prepared from 1 mol of *rac*-[Co(en)$_3$]Br_3 and *x* mol (x=1) of Ag_2(*d*-H_2tart) lies on R_2 (Fig. 11), in equilibrium with the partially resolved compound *Λ*-[Co(en)$_3$]$_{0.48}$·*Δ*-[Co(en)$_3$]$_{0.52}$(*d*-$H_2tart)_{1.5}$·5H_2O, but not with the solid *Λ*-[Co(en)$_3$]Br(*d*-H_2tart)·5H_2O. In the case of $0.43<x<0.97$, the isothermal concentration in equilibrium at 25 °C would enable us to attain perfect optical resolution.

The authors are grateful to Dr. Takasuke Matsuo and Mr. Yoshichika Yoshioka, Osaka University, for their advice and use of the DTA apparatus.

References

1) A. Fuyuhiro, K. Yamanari, and Y. Shimura, *Bull. Chem. Soc. Jpn.*, **52**, 90 (1979).
2) A. Fuyuhiro, K. Yamanari, and Y. Shimura, *Bull. Chem. Soc. Jpn.*, **52**, 2261 (1979).
3) A. Werner, *Chem. Ber.*, **45**, 121 (1912).
4) J. A. Broomhead, F. P. Dwyer, and J. W. Hogarth, *Inorg. Synth.*, **6**, 186 (1960).
5) H. Yoneda, K. Miyoshi, S. Suzuki, and T. Taura, *Bull. Chem. Soc. Jpn.*, **47**, 1661 (1974).
6) B. Norden, *Acta. Chem. Scand.*, **26**, 111 (1972).
7) A. Werner and M. Basyrin, *Chem. Ber.*, **46** 3230 (1913).
8) K. Yamanari, J. Hidaka, and Y. Shimura, *Bull. Chem. Soc. Jpn.*, **46**, 3724 (1973).
9) Y. Shimura and K. Tsutsui, *Bull. Chem. Soc. Jpn.*, **50**, 145 (1977).
10) A. Fuyuhiro, K. Yamanari, and Y. Shimura, *Chem. Lett.*, **1978**, 1393; A. Fuyuhiro, K. Yamanari, and Y. Shimura, *Bull. Chem. Soc. Jpn.*, **52**, 1420 (1979).
11) H. Yoneda, G. Takemoto, and U. Sakaguchi, *Bull. Chem. Soc. Jpn.*, **47**, 513 (1974).